The cytokine GDF15 signals through a population of brainstem cholecystokinin neurons to mediate anorectic signalling

Amy A Worth[1], Rosemary Shoop[1], Katie Tye[1], Claire H Feetham[1], Giuseppe D'Agostino[1,2], Garron T Dodd[3], Frank Reimann[4], Fiona M Gribble[4], Emily C Beebe[5], James D Dunbar[5], Jesline T Alexander-Chacko[5], Dana K Sindelar[5], Tamer Coskun[5], Paul J Emmerson[5], Simon M Luckman[1]*

[1]Faculty of Biology, Medicine and Health, The University of Manchester, Manchester, United Kingdom; [2]Rowett Institute, University of Aberdeen, Aberdeen, United Kingdom; [3]School of Biomedical Sciences, The University of Melbourne, Victoria, Australia; [4]Institute of Metabolic Science, Addenbrooke's Hospital, Cambridge, United Kingdom; [5]Lilly Research Laboratories, Eli Lilly & Company, Indianapolis, United States

Abstract The cytokine, GDF15, is produced in pathological states which cause cellular stress, including cancer. When over expressed, it causes dramatic weight reduction, suggesting a role in disease-related anorexia. Here, we demonstrate that the GDF15 receptor, GFRAL, is located in a subset of cholecystokinin neurons which span the area postrema and the nucleus of the tractus solitarius of the mouse. GDF15 activates GFRAL[AP/NTS] neurons and supports conditioned taste and place aversions, while the anorexia it causes can be blocked by a monoclonal antibody directed at GFRAL or by disrupting CCK neuronal signalling. The cancer-therapeutic drug, cisplatin, induces the release of GDF15 and activates GFRAL[AP/NTS] neurons, as well as causing significant reductions in food intake and body weight in mice. These metabolic effects of cisplatin are abolished by pre-treatment with the GFRAL monoclonal antibody. Our results suggest that GFRAL neutralising antibodies or antagonists may provide a co-treatment opportunity for patients undergoing chemotherapy.

*For correspondence:
simon.luckman@manchester.ac.uk

Introduction

The cytokine, GDF15 (a member of the TGF-β cytokine family, also known as MIC-1 and NAG-1), is expressed in several tissues throughout the body and circulates in the bloodstream of healthy humans (*Bootcov et al., 1997*; *Tsai et al., 2018*; *Patel et al., 2019*). Plasma levels increase dramatically in a number of pathological states associated with cellular stress, including cancers, cardiac failure, chronic kidney disease, infection and obesity (*Patel et al., 2019*; *Welsh et al., 2003*; *Kempf et al., 2007*; *Ho et al., 2013*; *Bauskin et al., 2006*; *Luan et al., 2019*). Furthermore, over expression of GDF15 causes a dramatic reduction in food intake and weight loss (*Tsai et al., 2018*; *Johnen et al., 2007*; *Macia et al., 2012*; *Chrysovergis et al., 2014*; *Xiong et al., 2017*). Together, this has led to the supposition that GDF15 does not have a normal, physiological role but is, instead, secreted as an adaptive response to disease (*Patel et al., 2019*; *Luan et al., 2019*). This said, the transgenic knock out of GDF15 from the germline results in obesity, which could be interpreted that the cytokine has an alternative physiological function to regulate body weight (*Tsai et al., 2013*; *Low et al., 2017*; *Tran et al., 2018*).

The GDF15 receptor, GFRAL (GDNF-family receptor α-like) is located exclusively in a small population of cells in the in the area postrema (AP) and nucleus of the tractus solitarius (NTS) of the

mouse dorsomedial medulla oblongata, (*Mullican et al., 2017*; *Yang et al., 2017*; *Emmerson et al., 2017*; *Hsu et al., 2017*) a brainstem region containing a number of characterised neurons that previously have been linked with appetite regulation (*Luckman, 1992*; *Rinaman et al., 1993*; *Larsen et al., 1997*; *Lawrence et al., 2000*; *Luckman and Lawrence, 2003*; *Ellacott et al., 2006*; *D'Agostino et al., 2016*; *Roman et al., 2016*; *Frikke-Schmidt et al., 2019*). Administration of recombinant GDF15 reduces food intake, but not in GFRAL knock-out mice (*Mullican et al., 2017*; *Yang et al., 2017*; *Emmerson et al., 2017*; *Hsu et al., 2017*). It also induces the cellular activation marker, Fos protein, in GFRAL-positive cells in the AP/NTS, and in putative downstream targets in the pons and amygdala, (*Xiong et al., 2017*; *Hsu et al., 2017*; *Frikke-Schmidt et al., 2019*), whereas selective surgical lesioning of the AP/NTS blocks the anorexic effects of the peptide (*Tsai et al., 2014*). The absolute identity of the primary responsive neurons has not been determined. Although a small number of GFRAL-positive neurons contain immunoreactivity for the catecholaminergic marker, tyrosine hydroxylase (TH), (*Yang et al., 2017*) relatively few TH-positive neurons are activated by exogenous GDF15 (*Tsai et al., 2014*). We have extended these investigations and found that the highest proportion of GFRAL-positive neurons contain the neuropeptide transmitter, cholecystokinin (CCK). We demonstrate that GFRAL cells are a sub-population of CCK neurons, which respond to administration of GDF15 or the cancer therapeutic drug, cisplatin, but not to other anorectic signals. Additionally, the effect of GDF15 to inhibit food intake is abrogated by the targeted deletion of CCK-containing neurons in the AP/NTS or by pre-administration of a CCK receptor antagonist. A single injection of GDF15 causes marked conditioned taste and place aversions, suggesting a strong negative affect, as well as activating downstream pathways previously described as mediating anorexia. Lastly, since we can block GDF15- or cisplatin-induced anorexia by neutralising the GFRAL receptor with a selective monoclonal antibody, we suggest that the anorectic responses to disease and, potentially, their therapeutic treatment may be mediated by this distinct signalling pathway.

Results

GFRAL is localised to CCK-positive neurons in the AP/NTS

Mice expressing Cre recombinase under the control of neuropeptide genes, were crossed with a reporter mouse expressing enhanced Yellow Fluorescent Protein in a Cre-dependent fashion (Rosa26-eYFP), so that the double mutants expressed eYFP in discrete populations of CCK (*Taniguchi et al., 2011*), glutamate (VGlut2; gene *Slc17a6*), preproglucagon (PPG; gene *Gcg*) (*Parker et al., 2012*) or prolactin-releasing peptide (PrRP; gene *Prlh*) (*Dodd et al., 2014*) neurons in the AP/NTS. Using antibodies against GFRAL, eYFP and TH, we were able to characterise putative, GDF15-sensitive cells. In the mouse, GFRAL was expressed in a continuous grouping of cells in the AP, extending into the medial region of the NTS (*Figure 1A*), as noted previously by others (*Mullican et al., 2017*; *Yang et al., 2017*; *Emmerson et al., 2017*; *Hsu et al., 2017*). Although dense within the AP and more sparsely distributed in the NTS, there were similar numbers of GFRAL neurons in the two structures (20 ± 1 per section in both the AP and the NTS). 60% of GFRAL-immunoreactive cells in the AP co-localised with Cck^{Cre}::eYFP, though this proportion was 31% in the NTS (*Figure 1B* and summary in *Supplementary file 1*). We confirmed this pattern using RNAScope in situ hybridisation histology, which provided slightly higher values of 69% and 35% overlap in the AP and NTS, respectively (*Figure 1—figure supplement 1A* and *Supplementary file 1*). Thus, overall, the majority of GFRAL neurons are CCKergic. By comparison, dual immunohistochemistry revealed that 27% of GFRAL neurons in the AP and 45% in the NTS contained TH (*Figure 1B*). Overall, approximately, 15% of GFRAL neurons contained both CCK and TH (*Figure 1—figure supplement 1B*). At least 54% GFRAL neurons in the AP co-localised with $Slc17a6^{Cre}$::eYFP, which fits with the consensus that CCK neurons in this brain region are glutamatergic (*Figure 1—figure supplement 1C*). Finally, GFRAL cells were distinct from other NTS populations which contain either PrRP or PPG (*Figure 1B*), which themselves either form a separate sub-population of TH neurons (*Dodd and Luckman, 2013*) or overlap with other CCK cells (*Garfield et al., 2012*; *Figure 1—figure supplement 1D*), respectively. In conclusion, GFRAL cells appear to form a distinct subset of CCK neurons, a proportion of which also contain TH.
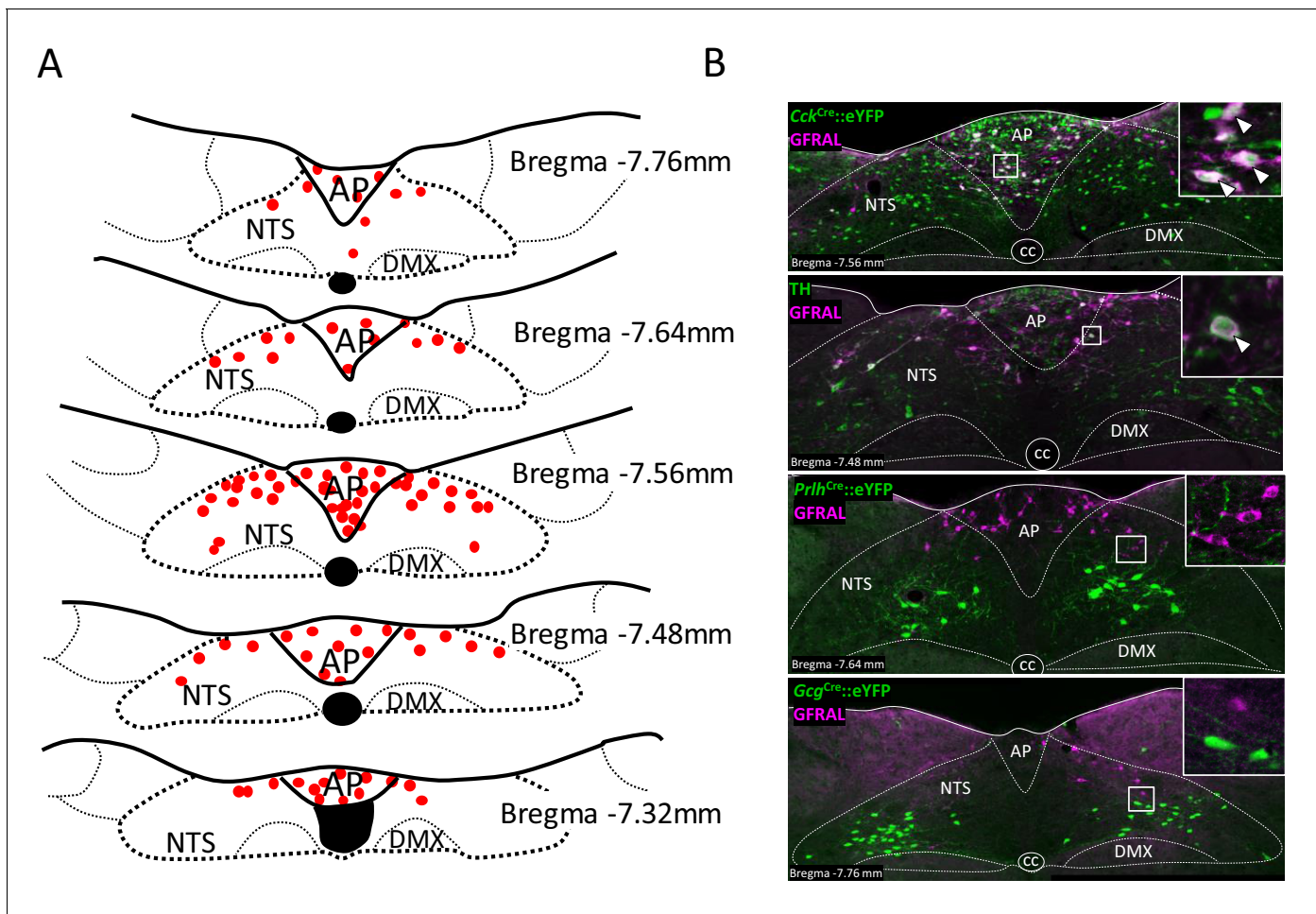
Figure 1. GFRAL-positive neurons in the AP and NTS co-localise with CCK. (**A**) Schematic describing the distribution of GFRAL-immunoreactive cell bodies in the AP and dorsal NTS at different rostrocaudal levels relative to *bregma*. (**B**) Dual-fluorescence labelling for GFRAL (magenta) with TH or eYFP (staining using antibody raised against green fluorescent protein) in three reporter mice, *Cck*Cre::eYFP, *Prlh*Cre::eYFP or *Gcg*Cre::eYFP. GFRAL co-localised with CCK and TH, but not PrRP or PPG (the latter being located more caudal to the majority of GFRAL neurons). White arrows in higher magnification inset indicate co-labelled cells. AP (area postrema), cc (central canal), DMX (dorsal motor nucleus of the tenth cranial nerve, vagus), NTS (nucleus of the tractus solitarius).

The online version of this article includes the following figure supplement(s) for figure 1:

Figure supplement 1. Further histological analysis of GFRAL/CCK neurons.

GDF15 produces anorexia and a negative affective valence

A single injection of GDF15 (2–8 nmol/kg, subcutaneous; s.c.) at lights-out produced a significant and dose-dependent decrease in normal, night-time feeding within 2 hr (hr) of administration (*Figure 2A*). Cumulative food intake had mostly recovered by 24 hr. This is within the range used by others who report dose-dependent effects of single, systemic injections of GDF15 in mice (*Patel et al., 2019*; *Mullican et al., 2017*). Doses of 4–8 nmol/kg were required to see a significant effect on fast-induced, day-time feeding (*Figure 2B*), and were the doses used in later experiments. Administration of GDF15 was associated with a negative affective valence, since a single injection supported a strong conditioned taste aversion (CTA) when paired with sucrose (see also *Patel et al., 2019*), and a conditioned place aversion (CPA) in mice (*Figure 2C and D*). In addition, pica behaviour, in which kaolin clay is consumed to remedy gastric malaise, was used as a measure of sickness given that rodents cannot vomit. Administration of GDF15 to rats on 3 consecutive days induced pica behaviour – a proxy for sickness behaviour – to an extent comparable to that seen following injection of the nausea-inducing toxin, lithium chloride (LiCl; *Figure 2—figure supplement 1*).
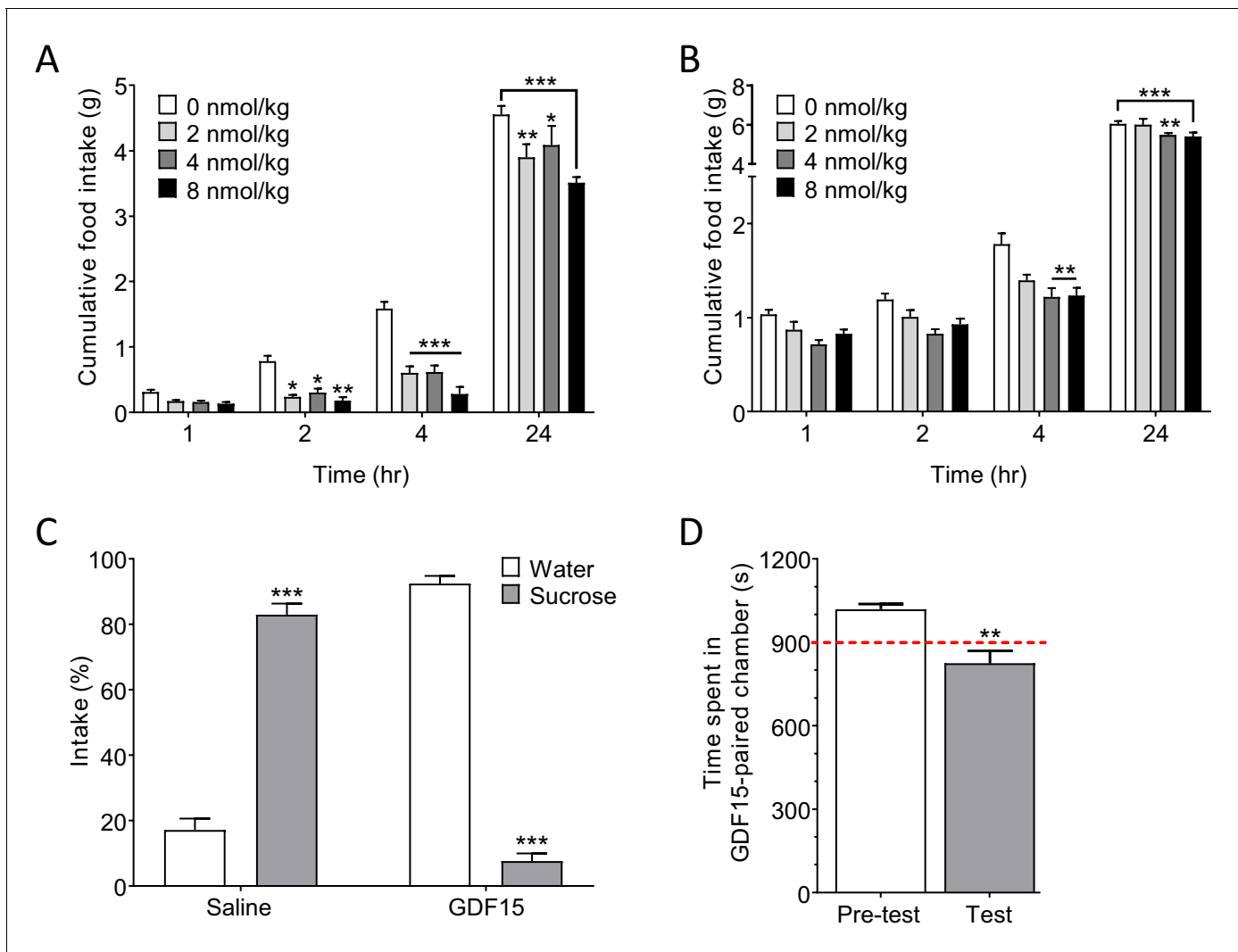
Figure 2. GDF15 produces anorexia and a negative affective valence. (**A**) Subcutaneous administration of GDF15, just before 'lights out,' decreased normal, night-time feeding (n = 6 per group; *p<0.05, **p<0.01, ***p<0.001, compared with 0 nmol/kg group; two-way ANOVA followed by Tukey's multiple comparison test). (**B**) GDF15 also decreased fast-induced, day-time re-feeding (n = 5–6 per group; **p<0.01, ***p<0.001, compared with 0 nmol/kg group). (**C**) GDF15 supported a conditioned taste aversion in mice when paired with sucrose as the conditioned stimulus. Data show two-bottle fluid intake 24 hr following a single conditioning to GDF15 (n = 6 per group; ***p<0.001, water versus sucrose intake for saline- and GDF15-treated groups; two-way ANOVA followed by Sidak's multiple comparison test). (**D**) GDF15 supported a conditioned place aversion in mice. Mice showed a preference for one side of the arena measured as time spent (seconds) in preferred side. During conditioning, mice received an injection of GDF15 on their preferred (dark) side and saline on their non-preferred side. On the test day, the mice displayed a decreased preference for the side on which they received GDF15 (n = 12; **p<0.01, time spent in preferred side; paired t-test).

The online version of this article includes the following figure supplement(s) for figure 2:

Figure supplement 1. GDF15 supports sickness behaviour in rats.

Together, these and recently published data (*Borner et al., 2020a*; *Borner et al., 2020b*) suggest that GDF15 is probably not a natural satiety factor, but exerts a pathophysiological action to cause anorexia. This conclusion is supported by the findings that circulating GDF15 levels do not correlate with meal times in humans, (*Patel et al., 2019*; *Tsai et al., 2015*) and that GDF15 knock out in mice does not result in significant changes in normal chow intake (*Tsai et al., 2013*; *Tran et al., 2018*).

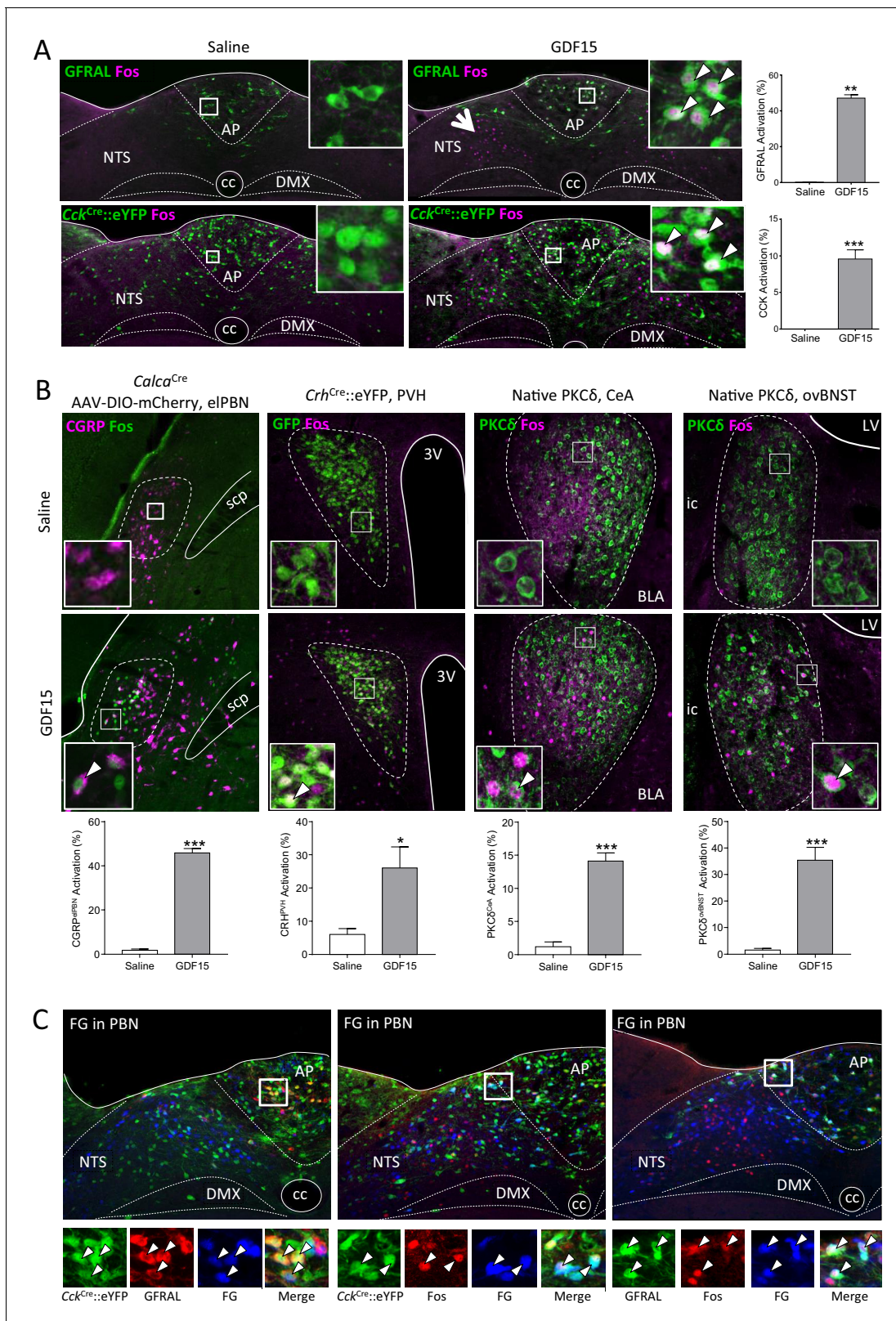## GDF15 activates CCK^{AP/NTS} neurons

Next, we determined the identity of GDF15-activated neurons by carrying out Fos-activity mapping in *Cck*^{Cre}::eYFP, *Prlh*^{Cre}::eYFP, *Gcg*^{Cre}::eYFP or *Pomc*^{eGFP} mice. A single, low-anorectic dose of GDF15 activated GFRAL+ve/CCK and TH neurons in the AP/NTS, as well as GFRAL-ve neurons at the same level of both the AP and NTS (*Figure 3A*; *Figure 3—figure supplement 1A and B*). Neither PrRP, PPG nor POMC neurons are activated significantly by GDF15 (*Figure 3—figure supplement 1B*). Thus, a very obvious group of GFRAL-ve cells in the medial NTS, that are activated by GDF15, remain unidentified (*Figure 3A*, arrow head). GFRAL cells are not activated by natural satiety signals acting after meal intake (*Figure 3—figure supplement 1C*); that is, following fast-induced re-feeding, the infusion of lipid directly into the stomach (300 µl Intralipid by gavage) or a low-dose of satiety-inducing, systemic CCK (6 µg/kg body weight, intraperitoneal; i.p.). Perhaps surprisingly, only a small number are activated by LiCl (128 mg/kg body weight, i.p.). This contrasts with the general activation profile of CCK neurons in the AP/NTS, which respond to different anorectic stimuli and which underlines that they are probably a mixed population (*D'Agostino et al., 2016*; *Roman et al., 2017*).

In terms of potential downstream mediators of the GDF15 signal, in addition to the non-GFRAL cells in the NTS and AP, significant increases in Fos staining were recorded in the lateral parabrachial nucleus of the pons (PBN), the paraventricular nucleus of the hypothalamus (PVH), the oval sub-nucleus of the bed nucleus of the stria terminalis (ovBNST) and in the central nucleus of the amygdala (CeA; *Figure 3—figure supplement 1D*). Using *Calca*^{Cre}::eYFP or *Crh*^{Cre}::eYFP mice, we show that some neurons in the PBN activated by GDF15 express calcitonin gene-related peptide (CGRP), while many in the PVH, but not the CeA and ovBNST, express corticotrophin-releasing hormone (CRH; *Figure 3B* and *Figure 3—figure supplement 1E*). Instead, within the ovBNST and CeA, a large proportion of Fos-positive cells contained PKC-δ immunoreactivity (*Figure 3B*). CCK^{NTS} neurons project directly to the PBN, including to cells containing CGRP (*Roman et al., 2016*; *Roman et al., 2017*); and, CCK$_1$ receptors in the PBN have been proposed to modulate information flow from gut to brain (*Mercer and Beart, 2004*; *Saleh et al., 1997*). CGRP^{PBN} neurons respond to a number of anorectic signals and may act as a point of convergence for different signalling pathways, themselves projecting forward to the CeA and elsewhere (*Wu et al., 2012*; *Carter et al., 2013*). Therefore, we used dual-fluorescence RNAScope to demonstrate the expression of *Cckr1* in the lateral PBN, but found the receptor mRNA in relatively few CGRP (*Calca* mRNA-expressing) cells (*Figure 3—figure supplement 1F*). Thus, CGRP neurons are unlikely to be the only target in the PBN for GFRAL neurons.

By repeating our Fos experiment but in mice previously injected with the retrograde tracer, Fluoro-Gold, into the lateral PBN, we demonstrate that both GFRAL and CCK neurons activated by GDF15 project directly to the PBN (*Figure 3C*). Likewise, CCK^{NTS} neurons also send direct projections to the PVH (*D'Agostino et al., 2016*). We confirmed this projection pattern using retrograde tracing, however, we showed that almost no GDF15-activated, GFRAL+ve or GFRAL-ve AP/NTS cells project directly to the PVH or to the ovBNST (*Figure 3—figure supplement 1G and H*). The most parsimonious conclusion is that GFRAL cells activated by GDF15 project directly to the PBN, which then activates downstream targets in the CeA, ovBNST and PVH. GFRAL cells may also synapse locally to activate other neuronal populations, including cells in the medial NTS. A very small number of these synaptically activated cells contain CCK or TH, and because almost none contain either PrRP, PPG or POMC, they may represent another distinct NTS phenotype. These GDF15-activated cells do not project to either the PBN or the ovBNST, but a few do project to the PVH. The others may represent local interneurons or potentially be responding to descending pathways.

Blocking CCK signalling attenuates the anorexia caused by GDF15

To confirm the importance of GFRAL/CCK^{AP/NTS} neurons in mediating the anorectic effects of GDF15, we used a recombinant adeno-associated virus (AAV) expressing a Cre-dependent designer pro-caspase and its activator, the Tobacco Etch Protease (flex-taCasp3-TEVp) to commit CCK^{AP/NTS} neurons to cell-autonomous apoptosis. *Cck*^{Cre}::eYFP mice were injected into the AP/NTS with the AAV-caspase or an AAV expressing mCherry to control for viral load and transduction efficiency. Post hoc examination confirmed that the designer caspase achieved an effective ablation of CCK^{AP/NTS} neurons, assessed by immunostaining for eYFP and also GFRAL (*Figure 4A* and *Figure 4—*

Figure 3. GDF15 activates GFRAL+ve/CCK neurons in the AP/NTS. (**A**) Fluorescence photomicrographs showing Fos expression (magenta) in GFRAL and CCK-positive neurons (green) in the AP/NTS following a minimal effective dose of GDF15. For triple labelling, see *Figure 3—figure supplement 1A*. The percentage of activated GFRAL-immunopositive or *Cck*Cre::eYFP neurons is presented on the right (n = 6–7 per group). White arrows in higher magnification insets indicate co-labelled cells. Note that GDF15 administration activated a group of cells in the medial NTS which are GFRAL-ve and

Figure 3 continued on next page

Figure 3 continued

CCK-ve (large arrow head). (**B**) Dual-label immunofluorescence for Fos and downstream neuronal targets. CGRP neurons were visualised by injecting *Calca*^{Cre} mice with AAV-DIO-mCherry (Fos green; CGRP magenta). In the other pictures, PKC-δ⁺ or *Crh*^{Cre}::eYFP cells are coloured green. Quantification is provided below the relevant photomicrographs (*Calca*^{Cre}n = 4 per group; *Crh*^{Cre} = 6–7 per group; PKC-δ⁺n = 6–7 per group). (**C**) GFRAL neurons, which were activated by GDF15, project directly to the parabrachial nucleus, as demonstrated using Fluoro-Gold retrotracing. White arrows in higher magnification insets indicate triple-labelled cells. aca (anterior part of the anterior commissure), AP (area postrema), BLA (basolateral amygdala), ovBNST (bed nucleus of the stria terminalis, oval sub-nucleus), cc (central canal), CeA (central nucleus of the amygdala), DMX (dorsal motor nucleus of the tenth cranial nerve, vagus), ic (internal capsule), LV (lateral ventricle), NTS (nucleus of the tractus solitarius), PBN (parabrachial nucleus), PVH (paraventricular nucleus of the hypothalamus), scp (superior cerebellar peduncle), 3V (third ventricle). *p<0.05, **p<0.01, ***p<0.001; unpaired t-test.

The online version of this article includes the following figure supplement(s) for figure 3:

Figure supplement 1. Neuronal activation by GDF15.

figure supplement 1). Over the 10-week period following viral injection, there was no significant difference in body weight between groups (*Figure 4—figure supplement 1*). However, whereas mice transduced with control AAV-mCherry responded to GDF15 with a significant decrease in night-time food intake, those bearing cell-specific ablation of CCK^{AP/NTS} neurons showed an abrogated response (*Figure 4B*). We further injected GDF15 into mice which had been pre-treated with the CCK receptor antagonist, devazepide. Compared with mice receiving a vehicle control injection, those receiving devazepide displayed an attenuated anorectic response to a subsequent single injection of GDF15 (*Figure 4C*). At early time points, the anorectic effect of GDF15 was reduced by approximately half.

GFRAL receptor blockade with a monoclonal antibody alleviates the adverse side effects of the cancer therapeutic drug, cisplatin

Finally, the platinum-based therapeutic drug, cisplatin, causes a long-term reduction in food intake, which can have a major contribution to mortality in cancer patients treated with the drug (*Dasari and Tchounwou, 2014*). There is recent evidence that cisplatin acts through the NTS → CGRP^{PBN} axis in both rats (*Alhadeff et al., 2015*; *Alhadeff et al., 2017*) and mice, (*Hsu et al., 2017*) and the latter study indicates that GFRAL knock-out mice are protected against the anorexic effects of cisplatin. In our hands, a single injection of cisplatin (4 mg/kg, i.p.) at the beginning of the dark phase, led to a reduction in both food intake and body weight which lasted for three days (*Figure 5A and B*). In the same animals, there was a significant increase in circulating GDF15, which also lasted for between 2 and 3 days (*Figure 5C*). After 1 day, GDF15 levels were 45 pg/ml and 270 pg/ml in vehicle- and cisplatin-treated mice, respectively. Food intake and weight loss at 2 days correlated directly with the plasma level of GDF15 (*Figure 5—figure supplement 1*). In a separate experiment, we found also that cisplatin at the same dose activated GFRAL^{AP/NTS} neurons, as assessed by Fos immunoreactivity (*Figure 5D*).

We have shown previously that weight loss induced in rats by a long-lasting recombinant GDF15 protein can be blocked by the single, subcutaneous administration of a selective monoclonal antibody raised against its receptor (GFRAL mAb) (*Emmerson et al., 2017*). Further, here we show that the reduction in food intake and body weight in mice, caused by three daily doses of native GDF15, is blocked by pre-administration of 10 mg/kg of the GFRAL mAb (*Figure 5E and F*). Importantly, this high dose of GFRAL mAb which effectively blocks GDF15 signalling, did not affect either food intake or body weight when injected alone, signifying that GFRAL is unlikely to have a role in either satiety signalling or normal energy balance (for full mAb dose-response data see *Figure 5—figure supplement 1*). Having determined an effective dose of the GFRAL mAb in mice, this was then used to investigate the role of GDF15/GFRAL signalling in mediating the effects of cisplatin. The GFRAL mAb was administered 1 day before cisplatin and, as before, by itself did not affect either food intake (*Figure 5G*) or body weight (*Figure 5H*). However, pre-administration of the GFRAL mAb completely blocked the anorectic action of cisplatin (*Figure 5G*) and prevented the cisplatin-induced body weight loss (*Figure 5H*).
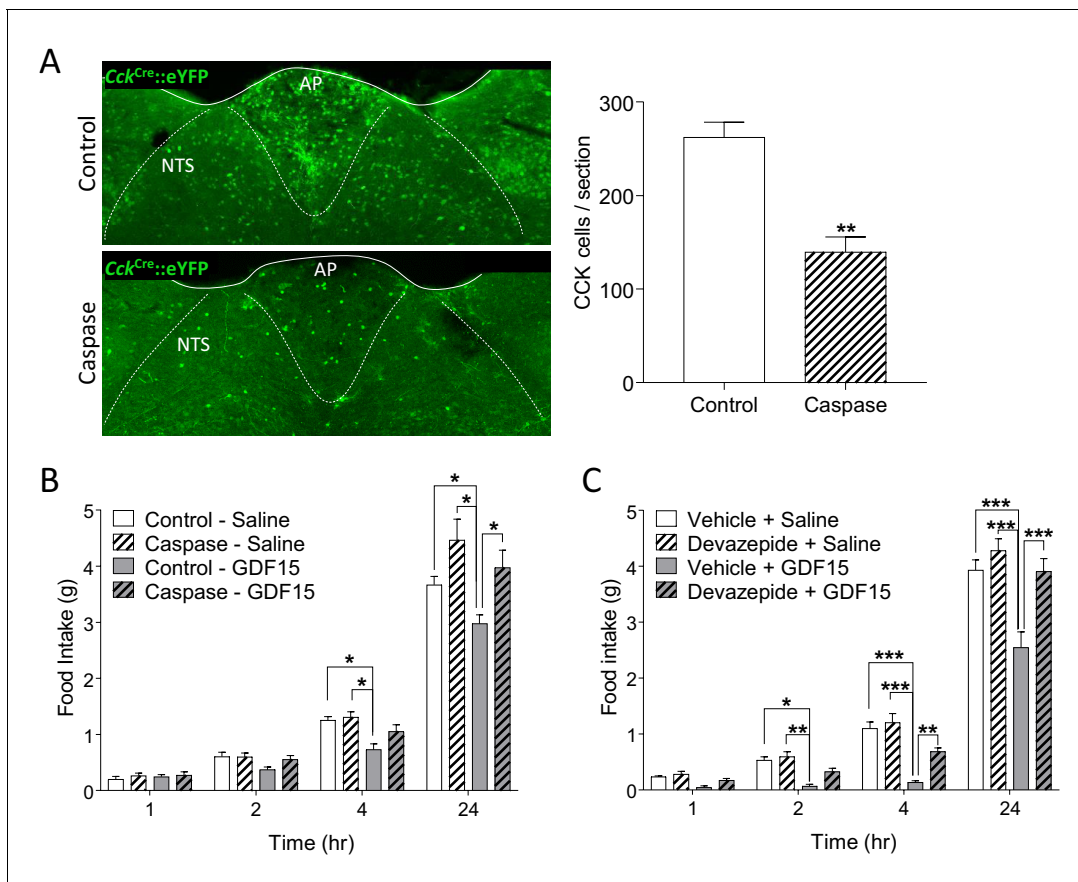
Figure 4. GDF15-induced anorexia is dependent on CCK signalling. (**A**) Injection of AAV-caspase into the AP and dorsal NTS of Cck^{Cre}::eYFP mice caused a reduction in the number of eYFP cells as assessed by immunohistochemistry (n = 7 per group; **p<0.01, unpaired t-test). (**B**) Cck^{Cre}::eYFP mice transduced with control AAV displayed a significant decrease in food intake following GDF15 administration, while those transduced with AAV-caspase showed reduced anorexia (n = 7 per group; *p<0.05; two-way ANOVA, followed by a post hoc Tukey test). (**C**) Pre-administration of the CCK receptor antagonist, devazepide, attenuated the anorectic response to GDF15 (n = 6 per group; *p<0.05, **p<0.01, ***p<0.001; two-way ANOVA, followed by a post hoc Tukey test).

The online version of this article includes the following figure supplement(s) for figure 4:

Figure supplement 1. Treatment with caspase leads to a significant loss of GFRAL neurons.

Discussion

The recent identification of the receptor for GDF15 and its localisation to a small population of cells in the dorsomedial medulla oblongata, an area involved in gut-brain signalling, ignited interest in the cytokine as having a potential role in body-weight regulation (*Mullican et al., 2017*; *Yang et al., 2017*; *Emmerson et al., 2017*; *Hsu et al., 2017*). Over expression of GDF15 leads to large reductions in both food intake and body weight (*Tsai et al., 2018*; *Johnen et al., 2007*; *Macia et al., 2012*; *Chrysovergis et al., 2014*; *Xiong et al., 2017*), whilst the obese phenotype reported for both the GDF15 and GFRAL knock-out mice is supporting evidence for a homeostatic role in normal body-weight regulation and, perhaps, satiety signalling (*Tsai et al., 2013*; *Low et al., 2017*; *Tran et al., 2018*; *Mullican et al., 2017*; *Hsu et al., 2017*). Careful examination of these null animals also provides results which would not be expected if this were the case. Thus, increases in food intake are either sex specific or only clearly apparent in mice fed high-energy diet. However, one of the more obvious phenotypes is a significant reduction in overall locomotor activity, which might explain a major part of the obesity (*Tsai et al., 2013*; *Tran et al., 2018*). Furthermore, the measurement of plasma levels of GDF15 in humans or mice does not correlate with meal times or nutritional status, which again would argue against it being a circulating satiety factor (*Patel et al., 2019*; *Tsai et al., 2015*). By contrast, GDF15 levels are greatly enhanced in a number of disease states,
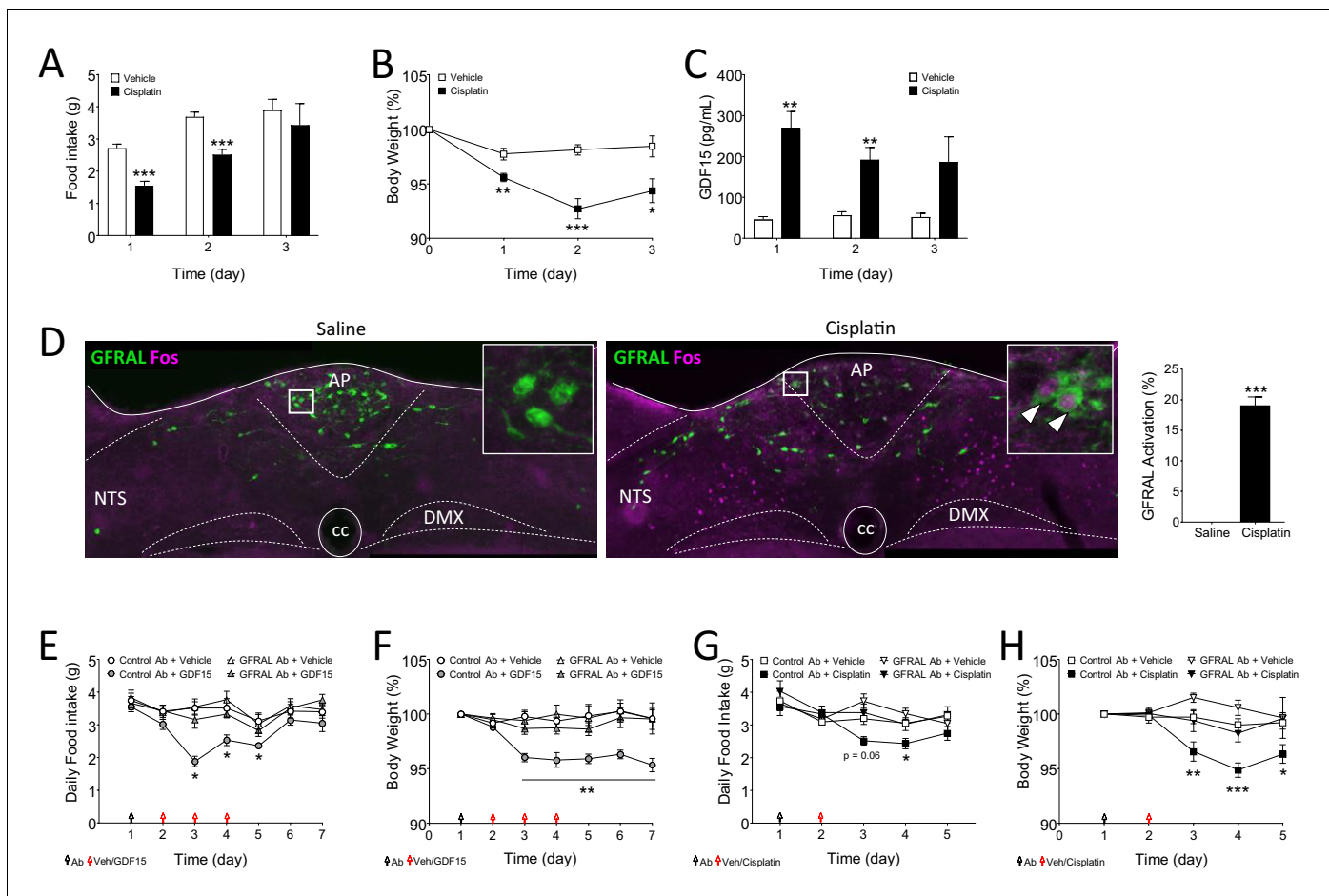
Figure 5. The anorectic action of the cancer therapeutic drug, cisplatin, is blocked by inhibition of signalling through GFRAL. (**A**) A single dose of cisplatin reduced food intake and (**B**) body weight over the following 3 days (n = 6 per time point; *p<0.05, **p<0.01, ***p<0.001; two-way ANOVA, followed by a post hoc Tukey test). (**C**) This corresponded with an increase in circulating GDF15 (n = 6 per time point, ***p<0.001, unpaired t-test) and (**D**) induction of Fos (magenta) in immunopositive GFRAL neurons (green) at 24 hr after administration (n = 5–6 per group; ***p<0.001, unpaired t-test). (**E**) Three injections of GDF15, on days 2–4, led to a decrease in cumulative food intake and (**F**) body weight (n = 6 per group; *p<0.05, **p<0.01; repeated measures ANOVA, followed by a post hoc Tukey test, control Ab + GDF15 versus all other groups). The actions of GDF15 were blocked completely by pre-administration of a monoclonal antibody against GFRAL (10 mg/kg) on day 1. The GFRAL mAb had no effect on food intake or body weight by itself. For full data set, using different concentrations of GFRAL mAb, see *Figure 5—figure supplement 1B and C*. (**G**) Pre-administration of 10 mg/kg GFRAL mAb the day before, completely blocked the reduction of food intake and (**H**) body weight caused by cisplatin (n = 5–6 per group; *p<0.05, **p<0.01, ***p<0.001; repeated measures ANOVA, followed by a post hoc Tukey test).

The online version of this article includes the following figure supplement(s) for figure 5:

Figure supplement 1. The anorectic action of the cancer therapeutic drug, cisplatin, is blocked by inhibition of signalling through GFRAL.

including cancer, cardiovascular disease and chronic kidney disease, pointing towards a more obvious role as a non-physiological anorectic signal (*Patel et al., 2019*; *Welsh et al., 2003*; *Kempf et al., 2007*; *Ho et al., 2013*; *Bauskin et al., 2006*; *Luan et al., 2019*). In fact, the only non-chronic disease situation described, in which GDF15 is up regulated, is *hyperemesis gravidarum* associated with intense nausea and vomiting in early pregnancy (*Fejzo et al., 2018*; *Petry et al., 2018*). Thus, while we will not rule out a physiological role for GDF15, most of the literature seems to point towards it having a more significant role in sickness behaviour. This is strongly supported by our results that show that systemic administration of GDF15 causes robust conditioned taste

aversion, conditioned place aversion and pica behaviour, and that blocking endogenous GFRAL signalling with a selective monoclonal antibody does not affect baseline food intake or body weight.

GFRAL-positive neurons span the AP and the inner border with the NTS, a region synonymous with responses to toxins and other nausea-inducing agents, and which lacks a blood-brain barrier (*Miller and Leslie, 1994*). The AP and NTS are also part of the dorsal vagal complex, which responds to gut-brain signalling. GFRAL is not expressed in the gut or in the vagus nerve, and since GDF15 is still effective at inducing anorexia in vagotomised rats, (*Yang et al., 2017*) the simplest conclusion is that circulating GDF15 acts directly on GFRAL expressed in the AP/NTS. We and others have argued for the existence of specific neuron types in this region of the brainstem which respond selectively to different sensory modalities (for example satiety versus nausea) in order to reduce food intake (*Luckman and Lawrence, 2003*; *Kreisler et al., 2014*). Thus, it is important to identify the phenotype of GFRAL cells. Although evidence has been provided that GFRAL is expressed in TH-positive catecholaminergic neurons, until now this has not been accurately quantified (*Yang et al., 2017*; *Tsai et al., 2014*). Here, using a variety of models, we conclude that the major, identifiable population of GFRAL neurons contain the neuropeptidergic transmitter, CCK. GFRAL-positive neurons respond to GDF15, but not with many other stimuli, and the action of GDF15 can be abrogated either by genetically ablating CCK neurons selectively in this region or by blocking CCK transmission. Thus, we propose that the primary target for GDF15 is a distinct population of GFRAL/CCK neurons which span the AP/NTS to engage well-characterised circuitry involved in anorexia and conditioned aversion (*Wu et al., 2012*; *Carter et al., 2013*; *Chen et al., 2018*). We have found that CCK neurons activated by GDF15 project directly to the PBN, and that other downstream targets, in the PVH, CeA and ovBNST are also involved. There is ample evidence for anorectic signals to utilise parallel downstream pathways, but with convergence at specific nodes which we demonstrate are activated by GDF15, including CGRP neurons in the PBN (*D'Agostino et al., 2016*; *Roman et al., 2016*; *Roman et al., 2017*) and/or PKC-δ^+ neurons in both the CeA and ovBNST (*Cai et al., 2014*; *Wang et al., 2019*). There is still much to learn about these pathways, not least because we have shown that GFRAL neurons are not activated by the archetypal nausea-inducing agent LiCl, nor does GDF15 activate PPG (here) or GLP-1 receptor neurons (*Welsh et al., 2003*; *Frikke-Schmidt et al., 2019*), both capable of transmitting nauseous signals. Recently, bacterial or viral infections have been associated with secretion of GDF15 and an adaptive response in order to increase pathogen tolerance (*Luan et al., 2019*). In this ground-breaking paper, it was demonstrated that GDF15/GFRAL signalling increases triglyceride production by the liver in order to protect tissues, which are dependent on triglycerides for fuel, from metabolic damage due to inflammation. Also, the loss of appetite and weight caused by metformin in diet-induced obese mice is dependent on GDF15/GFRAL signalling, as is the accompanying increase in insulin sensitivity (*Coll et al., 2020*).

It is interesting to note that increased GDF15 has been measured in the circulation of human cancer subjects (*Welsh et al., 2003*; *Bauskin et al., 2006*; *Brown et al., 2003*) and, recently an NTS → CGRP[PBN] → CeA/ovBNST axis has been implicated in mediating the anorexia associated with cancer models in mice (*Campos et al., 2017*). Likewise, work in rats has demonstrated that this pathway appears also to be activated by the platinum-based, cancer therapeutic drug, cisplatin (*Alhadeff et al., 2015*; *Alhadeff et al., 2017*). Although in neither case has the primary brainstem neuron been identified (*Hsu et al., 2017*), it is reported that weight loss caused by cisplatin is reduced in GFRAL knock-out mice, and we now show that this is true also if wild-type mice are pre-treated with a neutralising GFRAL antibody. Although it is yet to be verified, the possibility exists that both a disease state (cancer) and the treatment (cisplatin) may exacerbate anorexia through the same brainstem pathway. If this is the case, then either GFRAL neutralising antibodies or GFRAL antagonists may provide a possible co-treatment opportunity for patients suffering with cancer-related anorexia/cachexia. The caveat to this is that the secretion of GDF15 during cancer, as it appears so for inflammatory infections, is presumably an adaptive response, so blocking GDF15/GFRAL signalling may worsen the disease and other symptoms. GDF15 has been located in different tissues when they become cancerous (*Welsh et al., 2003*; *Buckhaults et al., 2003*). If GDF15 has an adaptive systemic effect, then it may be possible to bypass this and, instead, selectively target the central pathways downstream of brainstem GFRAL.

Materials and methods

Key resources table

Reagent type (species) or resource	Designation	Source or reference	Identifiers	Additional information
Genetic reagent (*Mus musculus*)	C57Bl/6J (Mouse, male)	Envigo	Stock #057	MGI:2164189
Genetic reagent (*Mus musculus*)	C57Bl/6NHsd (Mouse, male)	Envigo	Stock #044	MGI:2161078
Genetic reagent (*M. musculus*)	C57Bl/6J (Mouse, male)	Charles River	Stock #632	MGI:3028467
Genetic reagent (*M. musculus*)	C57Bl/6J (Mouse, male)	Janvier labs	N/A	MGI:2670020
Genetic reagent (*M. musculus*)	$Pomc^{eGFP}$ (Mouse, male)	Jackson Laboratories	Stock #: 009593	MGI:3851684
Genetic reagent (*M. musculus*)	$Cck^{ires-Cre}$ (Mouse, male)	Jackson Laboratories	Stock #: 012706	MGI:5014249
Genetic reagent (*M. musculus*)	$Crh^{ires-Cre}$ (Mouse, male)	Jackson Laboratories	Stock #: 012704	MGI:4452101
Genetic reagent (*M. musculus*)	$Slc17a6^{ires-Cre}$ (Mouse, male)	Jackson Laboratories	Stock #: 016963	MGI:5300532
Genetic reagent (*M. musculus*)	Rosa26-loxSTOPlox-eYFP (Mouse, male)	Jackson Laboratories	Stock #: 006148	MGI:3621481
Genetic reagent (*M. musculus*)	Gcg^{iCre} (Mouse, male)	*Parker et al., 2012* PMID:22638549	N/A	MGI:5432481
Genetic reagent (*M. musculus*)	$Prlh^{ires-Cre}$ (Mouse, male)	*Dodd et al., 2014* PMID:25176149	N/A	MGI:5634277
Genetic reagent (*M. musculus*)	$Calca^{Cre}$ (Mouse, male)	*Carter et al., 2013* PMID:24121436	N/A	MGI:5559692
Genetic reagent (Rattus norvegicus)	Sprague Dawley (Rat, male)	Envigo	Stock #: SD-002	N/A
Antibody	anti-cFos (Rabbit polyclonal)	Santa Cruz	Cat.# SC52 RRID:AB_2106783	Primary antibody (1:500) IHC
Antibody	anti-DS Red (Goat polyclonal)	Santa Cruz	Cat.# 33353 RRID:AB_639924	Primary antibody (1:500) IHC
Antibody	anti-GFP (Chicken polyclonal)	Abcam	Cat.# 13970 RRID:AB_300798	Primary antibody (1:2000) IHC
Antibody	anti-GFRAL (Sheep polyclonal)	Thermofisher	Cat.# PA5-47769 RRID:AB_2607220	Primary antibody (1:200) IHC
Antibody	anti-GLP1 (Rabbit polyclonal)	PenLabs	Cat.#. T-4363 RRID:AB_518978	Primary antibody (1:2000) IHC
Antibody	anti-PKCδ (Mouse monoclonal)	BD Biosciences	Cat.#. 610398 RRID:AB_397781	Primary antibody (1:500) IHC
Antibody	anti-TH (Rabbit polyclonal)	AbCam	Cat.# AB112 RRID:AB_297840	Primary antibody (1:2000) IHC
Antibody	anti-TH (Sheep polyclonal)	Millipore	Cat.# AB1542 RRID:AB_90755	Primary antibody (1:1000) IHC
Antibody	anti-chicken, Alexa Fluor 488 (Donkey polyclonal)	Jackson Immuno Research	Cat.# 703-545-155 RRID:AB_2340375	Secondary antibody (1:1000) IHC
Antibody	anti-mouse, Alexa Fluor 594 (Donkey polyclonal)	Jackson Immuno Research	Cat.# 715-585-150 RRID:AB_2340854	Secondary antibody (1:1000) IHC
Antibody	anti-rabbit, Alexa Fluor 350 (Donkey polyclonal)	Molecular Probes	Cat.# A10039 RRID:AB_2534015	Secondary antibody (1:1000) IHC
Antibody	anti-Sheep, Alexa Fluor 350 (Donkey polyclonal)	Molecular Probes	Cat.# A21097 RRID:AB_10376162	Secondary antibody (1:1000) IHC

Continued on next page

Continued

Reagent type (species) or resource	Designation	Source or reference	Identifiers	Additional information
Antibody	anti-sheep, Alexa Fluor 594 (Donkey polyclonal)	Molecular Probes	Cat.# A11016 RRID:AB_10562537	Secondary antibody (1:1000) IHC
Antibody	Anti-GFRAL (Mouse monoclonal)	*Emmerson et al., 2017* PMID:28846098	mIgG1 GFRAL 8A2	Subcutaneous injection (0–10 mg/kg)
Recombinant DNA reagent	AAV8-hSyn-DIO-mCherry	Dr Bryan Roth Addgene	Cat.# 50459-AAV8	N/A
Recombinant DNA reagent	AAV5-flex-taCasp3-TEVp	Dr Nirao Shah University of North Carolina Vector Core	N/A	PMID:23663785
Sequence-based reagent	*Gfral*	Advanced Cell Diagnostics	Cat.# 417021-C3	RNAScope mRNA probe
Sequence-based reagent	*Cck*	Advanced Cell Diagnostics	Cat.# 402271-C1	RNAScope mRNA probe
Sequence-based reagent	*Cckr1*	Advanced Cell Diagnostics	Cat.# 313751-C1	RNAScope mRNA probe
Sequence-based reagent	*Calca*	Advanced Cell Diagnostics	Cat.# 420361-C2	RNAScope mRNA probe
Peptide, recombinant protein	GDF15	R and D Systems	Cat.# 9279-GD	(4 nmol/kg)
Peptide, recombinant protein	Streptavadin 488	Jackson Immuno Research	Cat.# 016-540-084 RRID:AB_2337249	(1:1000) IHC
Peptide, recombinant protein	Streptavadin 594	Jackson Immuno Research	Cat.# 016-580-084 RRID:AB_2337250	(1:1000) IHC
Commercial assay or kit	Mouse/rat GDF15 ELISA	R and D Systems	Cat.# MGD-150	N/A
Commercial assay or kit	RNAscope Multiplex Fluorescent Assay	Advanced Cell Diagnostics	Cat # 323100	
Chemical compound, drug	Devazepide	Tocris Bioscience	Cat.# 2304	(1 mg/kg)
Chemical compound, drug	Lithium chloride (LiCl)	Sigma	Cat L9650 (mouse) Cat.# 73036 (rat)	Mouse (128 mg/kg) Rat (128 mg/kg)
Chemical compound, drug	Hydroxystibamidine (Fluoro-Gold)	Invitrogen, Thermofisher	Cat.# H22845	4% in H_2O
Chemical compound, drug	Cisplatin	Sigma Aldrich	Cat.# PHR1624	(4 mg/kg)
Software, algorithm	Prism	GraphPad	RRID:SCR_002798	Version 7
Software, algorithm	Fiji	ImageJ	RRID:SCR_002285	Version 2.0.0-rc-69/1.52 p
Software, algorithm	Micromanager	ImageJ	RRID:SCR_016865	Version 1.4.23
Software, algorithm	Smart	Panlab, Harvard Biosciences/Biochrom Ltd	RRID:SCR_002852	Version 3.0

Animals

Non-transgenic C57Bl/6 mice were obtained from Charles River (Manston, Kent, UK), Envigo (Huntingdon, UK and Indianapolis IN) or Janvier Labs (Le Genest-Saint-Isle, France). Pomc[eGFP], Cck[ires-Cre], Crh[ires-Cre] (*Taniguchi et al., 2011*), Slc17a6[ires-Cre] and Rosa26-loxSTOPlox-eYFP were all purchased from Jackson Laboratories (stock numbers 009593, 012706, 012704, 016963 and 006148, respectively; Bar Harbor, ME). We have described the generation of the PPG (Gcg[Cre]) and PrRP (Prlh[ires-Cre]) mice (*Parker et al., 2012*; *Dodd et al., 2014*). Calca[ires-Cre] mice (*Carter et al., 2013*) were a kind gift from Prof Richard Palmiter (Howard Hughes Medical Institute, University of Washington).

Drugs and viruses

Recombinant human GDF15 was either made in house as described (*Emmerson et al., 2017*) or purchased from R and D Systems (Abingdon, UK). GDF15 was initially dissolved in 15 mM HCl, neutralised and diluted in saline. Devazepide was purchased from Tocris Bioscience (Bristol, UK) and dissolved in 40% DMSO. Cisplatin (Sigma-Aldrich, Gillingham, UK) was dissolved directly in saline.

Fluoro-Gold (hydroxystilbamidine, 4% w/v solution in water; Invitrogen, ThermoFisher, MA) was injected into mice anaesthetised with isoflurane (2–3% in oxygen) and placed in a stereotaxic frame. The skull was exposed and holes drilled at the site of injection. Fluoro-Gold was delivered unilaterally via a glass micropipette affixed to a Nanoject II Auto Nanoliter Injector (Drummond Scientific Company, PA) using co-ordinates as determined in the Mouse Brain Atlas: (*Paxinos and Franklin, 2004*) elPBN, −4.9 mm A/P, −1.4 mm M/L, −3.8 mm D/V from *bregma* (12 nl); ovBNST, +0.3 mm A/P, −1.0 mm M/L, −4.5 mm D/V (18 nl); PVH, - 0.7 mm A/P; −0.3 mm M/L; −5.5 mm D/V (18 nl). All animals were left to recover for 2 weeks to allow axonal transport before being transcardially perfused (see below).

Viral injections into the AP/NTS were performed as described previously with minor modifications (*D'Agostino et al., 2016*; *D'Agostino et al., 2018*). Briefly, 9- to 11-week-old male mice were anaesthetised with a mixture of ketamine and xylazine dissolved in saline (80 and 10 mg/kg, respectively; 10 ml/kg i.p.). Mice were placed in a stereotaxic frame, an incision was made at the level of the *cisterna magna,* and neck muscles were carefully retracted. Following *dura* incision, the *obex* served as reference point for injections with a glass micropipette. AP/NTS coordinates were approximatively 0.2 mm A/P, 0 and ±0.2 mm M/L, −0.2 mm D/V from *obex*. About 150 nl of virus were delivered during each of the three microinjections. Animals were administered analgesia (5 mg/kg Carprofen, s.c.) for 2 days post-operatively and given a minimum of 14 days recovery before nighttime feeding measurement. AAV5-mCherry and AAV5-flex-taCasp3-TEVp were obtained from Addgene (Watertown, MA) and the University of North Carolina Vector Core (Chapel Hill, NC), respectively.

Tissue preparation and histology

For all immunohistochemical experiments, animals were deeply anaesthetised with 4% isoflurane in oxygen and transcardially perfused with heparinsed saline (20,000U per litre in 0.9% NaCl) followed by 4% paraformaldehyde in 0.1 M phosphate buffer. Brains were dissected and post-fixed overnight at 4℃ and then cryoprotected in 30% sucrose. Brains were cut into 30-µm-thick coronal sections using a freezing sledge microtome (Bright 8000, Cambridge, UK) and either processed immediately or stored in cryoprotectant solution at −20℃.

Immunohistochemistry was performed on free-floating sections at room temperature unless stated otherwise. All antibodies are listed in the Key Resource Table. Brain sections were washed in 0.2% Triton X-100 in 0.1 M phosphate buffer and blocked in 5% normal serum for 1 hr, before being incubated in primary antibody (made up in to 1% normal serum) overnight at 4℃. The next day, sections were washed again and then incubated in secondary antibody for 2 hr. Sections were washed and, where biotinylated secondary antibodies were used, incubated for a further hour in streptavidin-conjugated fluorophores diluted in phosphate buffer. Finally, sections were washed in water, mounted onto glass slides, air-dried overnight and coverslipped with ProLong Gold (Thermo Fisher Scientific, MA). Sections were visualised on a Zeiss Axiomanager.D2 upright microscope (Zeiss, Oberkochen, Germany) and images captured using a Coolsnap HQ1 camera (Photometics, AZ) through Micromanager software v1.4.23 (https://imagej.net/Micro-Manager). Specific band pass filter sets for DAPI, FITC and Texas Red were used to prevent bleed through from one channel to the next. All images were processed and analysed in Fiji ImageJ (https://fiji.sc/).

Eight-week-old C57BL/6J mice (n = 3) were anaesthetised by CO_2, decapitated, and the brains removed and snap frozen on crushed dry ice. Four or five 10-µm-thick tissue sections at the level of the AP or PBN were collected for RNA in situ hybridisation histology for *Gfral* (cat#417021-C3) and *Cck* (cat# 402271-C1) or *Cckr1* (cat#313751-C1) and *Calca* (cat#420361-C2), respectively. mRNA was detected using RNAscope Multiplex Fluorescent Assay reagent kits (Advanced Cell Diagnostics, Inc, Newark, CA), according to the manufacturer's instructions, at Gubra (Hørsholm, Denmark). Slides were counter stained with DAPI to identify cellular nuclei. Slides were scanned under a 20X objective in an Olympus VS120 Fluorescent scanner.

Feeding and body-weight studies

For GDF15 night-time feeding experiments, food was removed from the animals for 2 hr before lights out. At lights out, mice were administered GDF15 subcutaneously and food was returned at the same time. Food intake was recorded at 0, 1, 2, 4, and 24 hr after injection of GDF15. Devazepide (1 mg/kg, i.p) was administered 45 min before GDF15. For the fast-refeeding experiment, food was removed from the mice at lights out on the night before the experiment. After a 16.5 hr fast, mice were administered GDF15 and food returned. Food intake was measured at the same time points (n = 5–7 per group).

C57Bl/6J male mice (aged 10 = 18 weeks; n = 6 for each group) were administered a single, intraperitoneal dose of saline or cisplatin (4 mg/kg). Food intake and body weight were monitored daily. At 24, 48, and 72 hr, n = 6 mice from each group were sacrificed with CO_2 inhalation and blood was collected with cardiac puncture. Plasma was taken with Approtinin and DPP4 inhibitors. GDF15 levels are measured using a mouse specific ELISA, according to manufacturer's directions (R and D Systems, MGD150). A dose-finding experiment for GFRAL mAb (mIgG1 GFRAL 8A2, Lilly Indianapolis, USA) was performed. Briefly, 1 day prior to GDF15 administration at 4 nmol/kg for 3 consecutive days, the mice were subcutaneously dosed once either with control antibody (mIgG1 antibody, Lilly Indianapolis) at 10 mg/kg or ascending doses of antibody at 0.3, 1, 3 and 10 mg/kg of GFRAL mAb. Daily food intake and body weight were measured for three days. In a different experiment, control antibody or GFRAL mAb (both 10 mg/kg) were subcutaneously dosed once 1 day prior to intraperitoneal dose of cisplatin at 4 mg/kg.

Conditioned taste and place aversion tests, pica behaviour

For conditioned taste aversion, C57Bl/6J mice were housed in cages that permitted ad libitum access to water from two bottles, side-by-side, for at least 1 week before the experiment. On day 1 of the study, animals were water deprived overnight for 16.5 hr. The following morning (day 2), water-deprived animals were provided with two bottles of a novel 15% sucrose solution (dissolved in drinking water) for 30 min. At the end of the 30 min sucrose exposure, animals received an s.c. injection of either saline or GDF15 (4 nmol/kg, 4 ml/kg; n = 6 per group). Two water bottles were returned immediately and mice had unlimited access to water for one night. On day 3, mice were again water deprived overnight. On day 4, water-deprived animals were provided with one bottle of 15% sucrose and one bottle of water for a period of 24 hr. Volumes of sucrose and water intake were measured at 2 hr and 24 hr and used to calculate sucrose preference (sucrose intake/total fluid intake * 100). Food was available ad libitum throughout the study. The positioning of the sucrose and water bottles (left or right) was randomised within treatment groups.

Conditioned place aversion was performed using an apparatus composed of two chambers with distinct visual and tactile qualities, connected by a brightly lit corridor (Harvard Biosciences/Biochrom Ltd., Cambridge, UK). The darker chamber consisted of a rough black floor and black spotted walls, whereas the lighter chamber consisted of a smooth grey floor and grey striped walls. Time spent in each chamber was monitored by video cameras mounted directly above the apparatus, connected to a computer running tracking software (Smart v3.0, Panlab, Harvard Biosciences/Biochrom Ltd.). All procedures were carried out between three and five hours after lights on. On day 1, C57Bl/6J mice (n = 12) were given free access to the full apparatus and allowed to freely explore both chambers for 30 min. Their initial pre-test preference was calculated from the time spent in each chamber. A biased design was used, whereby GDF15 was associated with the most-preferred chamber, which was the darker chamber for all mice. On days 2 and 3, a conditioning session was performed, where mice were restricted to one chamber following administration of either GDF15 (4 nmol/kg, injected s.c. on day 2) or saline (0.9% NaCl injected s.c. on day 3). Following each injection, mice were returned to their home cage for 10 min and then placed in the relevant chamber for 30 min. On day 4, a test session was performed in identical fashion to day 1, and their post-conditioning preference was calculated from the time spent in each chamber. Food and water was available ad libitum throughout the study, except for when mice were in the conditioning apparatus.

To measure pica behaviour, male Sprague-Dawley rats (Envigo, Indianapolis, IN) were acclimated with kaolin pellets available ad libitum in a hopper placed continuously in the home cage. Rats were assigned randomly to three groups (n = 9–10 per group) and treated on 3 consecutive days with vehicle (acetate buffer, pH 5.5, 1 ml/kg, s.c.), human recombinant GDF15 (0.2 mg/kg, s.c.) or LiCl

(0.3 M in water, 1% body weight, equivalent to 128 mg/kg, i.p.). Body weight, chow and kaolin intake were determined daily.

Statistics

Statistical analyses were performed using Prism 7 (Graphpad Software, La Jolla, CA). Data were analysed using t-test, one-way ANOVA, two-way or repeated measures ANOVA with post hoc comparisons. When appropriate, non-parametric equivalents were used. N represents independent biological replicates. No statistical methods were used to predetermine sample sizes. Sample size was computed based on pilot data and published literature. Data are presented as mean ± SEM and statistical significance was set at $p < 0.05$.

Additional information

Competing interests

Emily C Beebe, James D Dunbar, Jesline T Alexander-Chacko, Dana K Sindelar, Tamer Coskun, Paul J Emmerson: Paid employee of Eli Lilly. Simon M Luckman: BB/S008098/1 is a BBSRC Industrial Partnership Award between SML and Eli Lilly. The other authors declare that no competing interests exist.

Funding

Author contributions

Amy A Worth, Conceptualization, Data curation, Formal analysis, Investigation, Visualization, Methodology, Writing - original draft, Writing - review and editing; Rosemary Shoop, Data curation, Formal analysis, Investigation, Visualization; Katie Tye, Emily C Beebe, James D Dunbar, Jesline T Alexander-Chacko, Dana K Sindelar, Formal analysis, Investigation; Claire H Feetham, Investigation; Giuseppe D'Agostino, Data curation, Formal analysis, Investigation, Methodology, Writing - review and editing; Garron T Dodd, Resources, Formal analysis, Investigation; Frank Reimann, Fiona M Gribble, Resources; Tamer Coskun, Paul J Emmerson, Resources, Formal analysis, Investigation, Methodology, Writing - review and editing; Simon M Luckman, Conceptualization, Resources, Supervision, Funding acquisition, Methodology, Writing - original draft, Project administration, Writing - review and editing

Author ORCIDs

Amy A Worth (iD) https://orcid.org/0000-0003-2573-7140
Rosemary Shoop (iD) https://orcid.org/0000-0002-3617-4358
Simon M Luckman (iD) https://orcid.org/0000-0001-5318-5473

Ethics

Animal experimentation: All procedures were conducted in accordance with either: the United Kingdom Animals (Scientific Procedures) Act, 1986 (ASPA) and approved by the local animal welfare ethical review body (AWERB); the Eli Lilly Institutional Animal Care and Use Committee (IACUC) in accordance with the National Institutes of Health Guide for Care and Use of Laboratory Animals; or the University of Melbourne Animal Ethics Committee (1914919) and conformed to National Health & 8 Medical Research Council (Australia) guidelines regarding the care and use of experimental animals. Additional guidance from the UK National Centre for 3R's (NC3Rs) was followed where applicable.

Decision letter and Author response

Decision letter https://doi.org/10.7554/eLife.55164.sa1
Author response https://doi.org/10.7554/eLife.55164.sa2

Additional files

Supplementary files

• Supplementary file 1. A summary table of the quantification of cell counts demonstrating neuropeptide co-expression in the medulla oblongata. The number of cells per section single-, double- or triple-labelled on sections through the AP and NTS. Values are stated as are mean ± SEM (n = number of animals). Percentage co-expression is written in the text. Methods involved either immunohistochemistry (top) or in situ hybridisation histology (bottom).

• Transparent reporting form

Data availability

All data generated or analysed during this study are included in the manuscript and supporting files.

References

Alhadeff AL, Holland RA, Nelson A, Grill HJ, De Jonghe BC. 2015. Glutamate receptors in the central nucleus of the amygdala mediate Cisplatin-Induced malaise and energy balance dysregulation through direct hindbrain projections. *Journal of Neuroscience* **35**:11094–11104. DOI: https://doi.org/10.1523/JNEUROSCI.0440-15.2015, PMID: 26245970

Alhadeff AL, Holland RA, Zheng H, Rinaman L, Grill HJ, De Jonghe BC. 2017. Excitatory Hindbrain-Forebrain communication is required for Cisplatin-Induced anorexia and weight loss. *The Journal of Neuroscience* **37**:362–370. DOI: https://doi.org/10.1523/JNEUROSCI.2714-16.2016, PMID: 28077715

Bauskin AR, Brown DA, Kuffner T, Johnen H, Luo XW, Hunter M, Breit SN. 2006. Role of macrophage inhibitory cytokine-1 in tumorigenesis and diagnosis of Cancer. *Cancer Research* **66**:4983–4986. DOI: https://doi.org/10.1158/0008-5472.CAN-05-4067, PMID: 16707416

Bootcov MR, Bauskin AR, Valenzuela SM, Moore AG, Bansal M, He XY, Zhang HP, Donnellan M, Mahler S, Pryor K, Walsh BJ, Nicholson RC, Fairlie WD, Por SB, Robbins JM, Breit SN. 1997. MIC-1, a novel macrophage inhibitory cytokine, is a divergent member of the TGF-beta superfamily. *PNAS* **94**:11514–11519. DOI: https://doi.org/10.1073/pnas.94.21.11514, PMID: 9326641

Borner T, Shaulson ED, Ghidewon MY, Barnett AB, Horn CC, Doyle RP, Grill HJ, Hayes MR, De Jonghe BC. 2020a. GDF15 induces anorexia through nausea and Emesis. *Cell Metabolism* **31**:351–362. DOI: https://doi.org/10.1016/j.cmet.2019.12.004

Borner T, Wald HS, Ghidewon MY, Zhang B, Wu Z, De Jonghe BC, Breen D, Grill HJ. 2020b. GDF15 induces an aversive visceral malaise state that drives anorexia and weight loss. *Cell Reports* **31**:107543. DOI: https://doi.org/10.1016/j.celrep.2020.107543, PMID: 32320650

Brown DA, Ward RL, Buckhaults P, Liu T, Romans KE, Hawkins NJ, Bauskin AR, Kinzler KW, Vogelstein B, Breit SN. 2003. MIC-1 serum level and genotype: associations with progress and prognosis of colorectal carcinoma. *Clinical Cancer Research* **9**:2642–2650. PMID: 12855642

Buckhaults P, Zhang Z, Chen YC, Wang TL, St Croix B, Saha S, Bardelli A, Morin PJ, Polyak K, Hruban RH, Velculescu VE, Shih I. 2003. Identifying tumor origin using a gene expression-based classification map. *Cancer Research* **63**:4144–4149. PMID: 12874019

Cai H, Haubensak W, Anthony TE, Anderson DJ. 2014. Central amygdala PKC-δ(+) neurons mediate the influence of multiple anorexigenic signals. *Nature Neuroscience* **17**:1240–1248. DOI: https://doi.org/10.1038/nn.3767, PMID: 25064852

Campos CA, Bowen AJ, Han S, Wisse BE, Palmiter RD, Schwartz MW. 2017. Cancer-induced anorexia and malaise are mediated by CGRP neurons in the parabrachial nucleus. *Nature Neuroscience* **20**:934–942. DOI: https://doi.org/10.1038/nn.4574, PMID: 28581479

Carter ME, Soden ME, Zweifel LS, Palmiter RD. 2013. Genetic identification of a neural circuit that suppresses appetite. *Nature* **503**:111–114. DOI: https://doi.org/10.1038/nature12596, PMID: 24121436

Chen JY, Campos CA, Jarvie BC, Palmiter RD. 2018. Parabrachial CGRP neurons establish and sustain aversive taste memories. *Neuron* **100**:891–899. DOI: https://doi.org/10.1016/j.neuron.2018.09.032, PMID: 30344042

Chrysovergis K, Wang X, Kosak J, Lee S-H, Kim JS, Foley JF, Travlos G, Singh S, Baek SJ, Eling TE. 2014. NAG-1/GDF-15 prevents obesity by increasing thermogenesis, lipolysis and oxidative metabolism. *International Journal of Obesity* **38**:1555–1564. DOI: https://doi.org/10.1038/ijo.2014.27

Coll AP, Chen M, Taskar P, Rimmington D, Patel S, Tadross JA, Cimino I, Yang M, Welsh P, Virtue S, Goldspink DA, Miedzybrodzka EL, Konopka AR, Esponda RR, Huang JT, Tung YCL, Rodriguez-Cuenca S, Tomaz RA, Harding HP, Melvin A, et al. 2020. GDF15 mediates the effects of metformin on body weight and energy balance. *Nature* **578**:444–448. DOI: https://doi.org/10.1038/s41586-019-1911-y, PMID: 31875646

D'Agostino G, Lyons DJ, Cristiano C, Burke LK, Madara JC, Campbell JN, Garcia AP, Land BB, Lowell BB, Dileone RJ, Heisler LK. 2016. Appetite controlled by a cholecystokinin nucleus of the solitary tract to hypothalamus neurocircuit. *eLife* **5**:e12225. DOI: https://doi.org/10.7554/eLife.12225, PMID: 26974347

D'Agostino G, Lyons D, Cristiano C, Lettieri M, Olarte-Sanchez C, Burke LK, Greenwald-Yarnell M, Cansell C, Doslikova B, Georgescu T, Martinez de Morentin PB, Myers MG, Rochford JJ, Heisler LK. 2018. Nucleus of the solitary tract serotonin 5-HT$_{2C}$receptors modulate food intake. *Cell Metabolism* **28**:619–630. DOI: https://doi.org/10.1016/j.cmet.2018.07.017, PMID: 30146485

Dasari S, Tchounwou PB. 2014. Cisplatin in Cancer therapy: molecular mechanisms of action. *European Journal of Pharmacology* **740**:364–378. DOI: https://doi.org/10.1016/j.ejphar.2014.07.025, PMID: 25058905

Dodd GT, Worth AA, Nunn N, Korpal AK, Bechtold DA, Allison MB, Myers MG, Statnick MA, Luckman SM. 2014. The thermogenic effect of leptin is dependent on a distinct population of prolactin-releasing peptide neurons in the dorsomedial hypothalamus. *Cell Metabolism* **20**:639–649. DOI: https://doi.org/10.1016/j.cmet.2014.07.022, PMID: 25176149

Dodd GT, Luckman SM. 2013. Physiological roles of GPR10 and PrRP signaling. *Frontiers in Endocrinology* **4**:20. DOI: https://doi.org/10.3389/fendo.2013.00020, PMID: 23467899

Ellacott KL, Halatchev IG, Cone RD. 2006. Characterization of leptin-responsive neurons in the caudal brainstem. *Endocrinology* **147**:3190–3195. DOI: https://doi.org/10.1210/en.2005-0877, PMID: 16601142

Emmerson PJ, Wang F, Du Y, Liu Q, Pickard RT, Gonciarz MD, Coskun T, Hamang MJ, Sindelar DK, Ballman KK, Foltz LA, Muppidi A, Alsina-Fernandez J, Barnard GC, Tang JX, Liu X, Mao X, Siegel R, Sloan JH, Mitchell PJ, et al. 2017. The metabolic effects of GDF15 are mediated by the orphan receptor GFRAL. *Nature Medicine* **23**:1215–1219. DOI: https://doi.org/10.1038/nm.4393, PMID: 28846098

Fejzo MS, Sazonova OV, Sathirapongsasuti JF, Hallgrímsdóttir IB, Vacic V, MacGibbon KW, Schoenberg FP, Mancuso N, Slamon DJ, Mullin PM, 23andMe Research Team. 2018. Placenta and appetite genes GDF15 and IGFBP7 are associated with hyperemesis gravidarum. *Nature Communications* **9**:1178. DOI: https://doi.org/10.1038/s41467-018-03258-0, PMID: 29563502

Frikke-Schmidt H, Hultman K, Galaske JW, Jørgensen SB, Myers MG, Seeley RJ. 2019. GDF15 acts synergistically with liraglutide but is not necessary for the weight loss induced by bariatric surgery in mice. *Molecular Metabolism* **21**:13–21. DOI: https://doi.org/10.1016/j.molmet.2019.01.003, PMID: 30685336

Garfield AS, Patterson C, Skora S, Gribble FM, Reimann F, Evans ML, Myers MG, Heisler LK. 2012. Neurochemical characterization of body Weight-Regulating leptin receptor neurons in the nucleus of the solitary tract. *Endocrinology* **153**:4600–4607. DOI: https://doi.org/10.1210/en.2012-1282

Ho JE, Hwang SJ, Wollert KC, Larson MG, Cheng S, Kempf T, Vasan RS, Januzzi JL, Wang TJ, Fox CS. 2013. Biomarkers of cardiovascular stress and incident chronic kidney disease. *Clinical Chemistry* **59**:1613–1620. DOI: https://doi.org/10.1373/clinchem.2013.205716, PMID: 23873716

Hsu JY, Crawley S, Chen M, Ayupova DA, Lindhout DA, Higbee J, Kutach A, Joo W, Gao Z, Fu D, To C, Mondal K, Li B, Kekatpure A, Wang M, Laird T, Horner G, Chan J, McEntee M, Lopez M, et al. 2017. Non-homeostatic body weight regulation through a brainstem-restricted receptor for GDF15. *Nature* **550**:255–259. DOI: https://doi.org/10.1038/nature24042, PMID: 28953886

Johnen H, Lin S, Kuffner T, Brown DA, Tsai VW, Bauskin AR, Wu L, Pankhurst G, Jiang L, Junankar S, Hunter M, Fairlie WD, Lee NJ, Enriquez RF, Baldock PA, Corey E, Apple FS, Murakami MM, Lin EJ, Wang C, et al. 2007. Tumor-induced anorexia and weight loss are mediated by the TGF-beta superfamily cytokine MIC-1. *Nature Medicine* **13**:1333–1340. DOI: https://doi.org/10.1038/nm1677, PMID: 17982462

Kempf T, Horn-Wichmann R, Brabant G, Peter T, Allhoff T, Klein G, Drexler H, Johnston N, Wallentin L, Wollert KC. 2007. Circulating concentrations of growth-differentiation factor 15 in apparently healthy elderly individuals and patients with chronic heart failure as assessed by a new immunoradiometric sandwich assay. *Clinical Chemistry* **53**:284–291. DOI: https://doi.org/10.1373/clinchem.2006.076828, PMID: 17185363

Kreisler AD, Davis EA, Rinaman L. 2014. Differential activation of chemically identified neurons in the caudal nucleus of the solitary tract in non-entrained rats after intake of satiating vs. non-satiating meals. *Physiology & Behavior* **136**:47–54. DOI: https://doi.org/10.1016/j.physbeh.2014.01.015, PMID: 24508750

Larsen PJ, Tang-Christensen M, Jessop DS. 1997. Central administration of glucagon-like peptide-1 activates hypothalamic neuroendocrine neurons in the rat. *Endocrinology* **138**:4445–4455. DOI: https://doi.org/10.1210/endo.138.10.5270, PMID: 9322962

Lawrence CB, Celsi F, Brennand J, Luckman SM. 2000. Alternative role for prolactin-releasing peptide in the regulation of food intake. *Nature Neuroscience* **3**:645–646. DOI: https://doi.org/10.1038/76597, PMID: 10862694

Low JK, Ambikairajah A, Shang K, Brown DA, Tsai VW, Breit SN, Karl T. 2017. First behavioural characterisation of a knockout mouse model for the transforming growth factor (TGF)-β superfamily cytokine, MIC-1/GDF15. *PLOS ONE* **12**:e0168416. DOI: https://doi.org/10.1371/journal.pone.0168416, PMID: 28081177

Luan HH, Wang A, Hilliard BK, Carvalho F, Rosen CE, Ahasic AM, Herzog EL, Kang I, Pisani MA, Yu S, Zhang C, Ring AM, Young LH, Medzhitov R. 2019. GDF15 is an Inflammation-Induced central mediator of tissue tolerance. *Cell* **178**:1231–1244. DOI: https://doi.org/10.1016/j.cell.2019.07.033, PMID: 31402172

Luckman SM. 1992. Fos-like immunoreactivity in the brainstem of the rat following peripheral administration of cholecystokinin. *Journal of Neuroendocrinology* **4**:149–152. DOI: https://doi.org/10.1111/j.1365-2826.1992.tb00152.x, PMID: 21554590

Luckman SM, Lawrence CB. 2003. Anorectic brainstem peptides: more pieces to the puzzle. *Trends in Endocrinology & Metabolism* **14**:60–65. DOI: https://doi.org/10.1016/S1043-2760(02)00033-4, PMID: 12591175

Macia L, Tsai VW, Nguyen AD, Johnen H, Kuffner T, Shi YC, Lin S, Herzog H, Brown DA, Breit SN, Sainsbury A. 2012. Macrophage inhibitory cytokine 1 (MIC-1/GDF15) decreases food intake, body weight and improves glucose tolerance in mice on normal & obesogenic diets. *PLOS ONE* **7**:e34868. DOI: https://doi.org/10.1371/journal.pone.0034868, PMID: 22514681

Mercer LD, Beart PM. 2004. Immunolocalization of CCK1R in rat brain using a new anti-peptide antibody. *Neuroscience Letters* **359**:109–113. DOI: https://doi.org/10.1016/j.neulet.2004.01.045, PMID: 15050723

Miller AD, Leslie RA. 1994. The area postrema and vomiting. *Frontiers in Neuroendocrinology* **15**:301–320. DOI: https://doi.org/10.1006/frne.1994.1012, PMID: 7895890

Mullican SE, Lin-Schmidt X, Chin CN, Chavez JA, Furman JL, Armstrong AA, Beck SC, South VJ, Dinh TQ, Cash-Mason TD, Cavanaugh CR, Nelson S, Huang C, Hunter MJ, Rangwala SM. 2017. GFRAL is the receptor for GDF15 and the ligand promotes weight loss in mice and nonhuman primates. *Nature Medicine* **23**:1150–1157. DOI: https://doi.org/10.1038/nm.4392, PMID: 28846097

Parker HE, Adriaenssens A, Rogers G, Richards P, Koepsell H, Reimann F, Gribble FM. 2012. Predominant role of active versus facilitative glucose transport for glucagon-like peptide-1 secretion. *Diabetologia* **55**:2445–2455. DOI: https://doi.org/10.1007/s00125-012-2585-2, PMID: 22638549

Patel S, Alvarez-Guaita A, Melvin A, Rimmington D, Dattilo A, Miedzybrodzka EL, Cimino I, Maurin AC, Roberts GP, Meek CL, Virtue S, Sparks LM, Parsons SA, Redman LM, Bray GA, Liou AP, Woods RM, Parry SA, Jeppesen PB, Kolnes AJ, et al. 2019. GDF15 provides an endocrine signal of nutritional stress in mice and humans. *Cell Metabolism* **29**:707–718. DOI: https://doi.org/10.1016/j.cmet.2018.12.016, PMID: 30639358

Paxinos G, Franklin KBJ. 2004. *The Mouse Brain in Stereotaxic Coordinates*. Elsevier Academic Press.

Petry CJ, Ong KK, Burling KA, Barker P, Goodburn SF, Perry JRB, Acerini CL, Hughes IA, Painter RC, Afink GB, Dunger DB, O'Rahilly S. 2018. Associations of vomiting and antiemetic use in pregnancy with levels of circulating GDF15 early in the second trimester: a nested case-control study. *Wellcome Open Research* **3**:123. DOI: https://doi.org/10.12688/wellcomeopenres.14818.1, PMID: 30345390

Rinaman L, Verbalis JG, Stricker EM, Hoffman GE. 1993. Distribution and neurochemical phenotypes of caudal medullary neurons activated to express cFos following peripheral administration of cholecystokinin. *The Journal of Comparative Neurology* **338**:475–490. DOI: https://doi.org/10.1002/cne.903380402, PMID: 8132858

Roman CW, Derkach VA, Palmiter RD. 2016. Genetically and functionally defined NTS to PBN brain circuits mediating anorexia. *Nature Communications* **7**:11905. DOI: https://doi.org/10.1038/ncomms11905, PMID: 27301688

Roman CW, Sloat SR, Palmiter RD. 2017. A tale of two circuits: CCK[NTS] neuron stimulation controls appetite and induces opposing motivational states by projections to distinct brain regions. *Neuroscience* **358**:316–324. DOI: https://doi.org/10.1016/j.neuroscience.2017.06.049, PMID: 28684275

Saleh TM, Kombian SB, Zidichouski JA, Pittman QJ. 1997. Cholecystokinin and neurotensin inversely modulate excitatory synaptic transmission in the parabrachial nucleus in vitro. *Neuroscience* **77**:23–35. DOI: https://doi.org/10.1016/S0306-4522(96)00463-0, PMID: 9044371

Taniguchi H, He M, Wu P, Kim S, Paik R, Sugino K, Kvitsiani D, Kvitsani D, Fu Y, Lu J, Lin Y, Miyoshi G, Shima Y, Fishell G, Nelson SB, Huang ZJ. 2011. A resource of cre driver lines for genetic targeting of GABAergic neurons in cerebral cortex. *Neuron* **71**:995–1013. DOI: https://doi.org/10.1016/j.neuron.2011.07.026, PMID: 21943598

Tran T, Yang J, Gardner J, Xiong Y. 2018. GDF15 deficiency promotes high fat diet-induced obesity in mice. *PLOS ONE* **13**:e0201584. DOI: https://doi.org/10.1371/journal.pone.0201584, PMID: 30070999

Tsai VW, Macia L, Johnen H, Kuffner T, Manadhar R, Jørgensen SB, Lee-Ng KK, Zhang HP, Wu L, Marquis CP, Jiang L, Husaini Y, Lin S, Herzog H, Brown DA, Sainsbury A, Breit SN. 2013. TGF-b superfamily cytokine MIC-1/GDF15 is a physiological appetite and body weight regulator. *PLOS ONE* **8**:e55174. DOI: https://doi.org/10.1371/journal.pone.0055174, PMID: 23468844

Tsai VW, Manandhar R, Jørgensen SB, Lee-Ng KK, Zhang HP, Marquis CP, Jiang L, Husaini Y, Lin S, Sainsbury A, Sawchenko PE, Brown DA, Breit SN. 2014. The anorectic actions of the tgfβ cytokine MIC-1/GDF15 require an

intact brainstem area postrema and nucleus of the solitary tract. *PLOS ONE* **9**:e100370. DOI: https://doi.org/10.1371/journal.pone.0100370, PMID: 24971956

Tsai VW, Macia L, Feinle-Bisset C, Manandhar R, Astrup A, Raben A, Lorenzen JK, Schmidt PT, Wiklund F, Pedersen NL, Campbell L, Kriketos A, Xu A, Pengcheng Z, Jia W, Curmi PM, Angstmann CN, Lee-Ng KK, Zhang HP, Marquis CP, et al. 2015. Serum levels of human MIC-1/GDF15 vary in a diurnal pattern, do not display a profile suggestive of a satiety factor and are related to BMI. *PLOS ONE* **10**:e0133362. DOI: https://doi.org/10.1371/journal.pone.0133362, PMID: 26207898

Tsai VWW, Husaini Y, Sainsbury A, Brown DA, Breit SN. 2018. The MIC-1/GDF15-GFRAL pathway in energy homeostasis: implications for obesity, cachexia, and other associated diseases. *Cell Metabolism* **28**:353–368. DOI: https://doi.org/10.1016/j.cmet.2018.07.018, PMID: 30184485

Wang Y, Kim J, Schmit MB, Cho TS, Fang C, Cai H. 2019. A bed nucleus of stria terminalis microcircuit regulating inflammation-associated modulation of feeding. *Nature Communications* **10**:2769. DOI: https://doi.org/10.1038/s41467-019-10715-x, PMID: 31235690

Welsh JB, Sapinoso LM, Kern SG, Brown DA, Liu T, Bauskin AR, Ward RL, Hawkins NJ, Quinn DI, Russell PJ, Sutherland RL, Breit SN, Moskaluk CA, Frierson HF, Hampton GM. 2003. Large-scale delineation of secreted protein biomarkers overexpressed in Cancer tissue and serum. *PNAS* **100**:3410–3415. DOI: https://doi.org/10.1073/pnas.0530278100, PMID: 12624183

Wu Q, Clark MS, Palmiter RD. 2012. Deciphering a neuronal circuit that mediates appetite. *Nature* **483**:594–597. DOI: https://doi.org/10.1038/nature10899, PMID: 22419158

Xiong Y, Walker K, Min X, Hale C, Tran T, Komorowski R, Yang J, Davda J, Nuanmanee N, Kemp D, Wang X, Liu H, Miller S, Lee KJ, Wang Z, Véniant MM. 2017. Long-acting MIC-1/GDF15 molecules to treat obesity: evidence from mice to monkeys. *Science Translational Medicine* **9**:eaan8732. DOI: https://doi.org/10.1126/scitranslmed.aan8732

Yang L, Chang CC, Sun Z, Madsen D, Zhu H, Padkjær SB, Wu X, Huang T, Hultman K, Paulsen SJ, Wang J, Bugge A, Frantzen JB, Nørgaard P, Jeppesen JF, Yang Z, Secher A, Chen H, Li X, John LM, et al. 2017. GFRAL is the receptor for GDF15 and is required for the anti-obesity effects of the ligand. *Nature Medicine* **23**:1158–1166. DOI: https://doi.org/10.1038/nm.4394, PMID: 28846099